

Physicochemical Properties of Silicate- and Oleate- Nanoparticles for Heavy Metal Removal Applications

(Sifat Fizikokimia bagi Nanozarah Silikat dan Oleat untuk Aplikasi Penyingkiran Logam Berat)

NORA'AINI ALI¹, LAILI CHE ROSE^{2*}, NUR RAFIQAH ABDUL RAZAK², NURUL SYAHIRAH AZMAN¹, NORHAFIZA ILYANA YATIM³ & NOR AZMAN KASAN³

¹*Faculty of Ocean Engineering Technology, University Malaysia Terengganu, 21030 Kuala Nerus, Terengganu, Malaysia*

²*Faculty of Science and Marine Environment, Universiti Malaysia Terengganu, 21030 Kuala Nerus, Terengganu, Malaysia*

³*Higher Institution Centre of Excellence (HICoE), Institute of Tropical Aquaculture and Fisheries, Universiti Malaysia Terengganu, 21030, Kuala Nerus, Terengganu, Malaysia*

Received: 3 September 2024/Accepted: 4 February 2025

ABSTRACT

Utilizing magnetic nanoparticles (MN) to extract heavy metal ions from wastewater is a promising method for metal recovery and can reduce secondary waste production. The objective of this study was to evaluate the changes in physicochemical characteristics of silicate-nanoparticles (MNs-SiO) and oleate-nanoparticles (MNs-C-COOH) prepared via the biocompatible W/O microemulsion technique. The characteristics and properties of MNs-SiO and MNs-C-COOH nanoparticles were investigated by Scanning Electron Microscope (SEM), Fourier Transform Infrared (FTIR), X-ray Diffraction (XRD), and Vibrating-sample magnetometer (VSM). The performance of this nanoparticles (MNs-SiO), and (MNs-C-COOH) (MNs-SiO), and (MNs-C-COOH) as adsorbents were evaluated for removal of selected heavy metal ions, nickel (Ni^{2+}), manganese (Mn^{2+}) and lead (Pb^{2+}) at different modification agent and pH. It was found that MNs-SiO adsorbent was highly favourable towards Pb^{2+} (673.4 mg/g) at pH 3, followed by Mn^{2+} (544.8 mg/g) and Ni^{2+} (182.43 mg/g) at pH 7, respectively. The MNs-C-COOH adsorbent indicated the high adsorption of Ni^{2+} , which was 254 mg/g at pH 6. For commercial magnetic nanoparticles adsorbent, showed high selection towards Pb^{2+} , 660.13 mg/g at pH 6 and other ions showed less than 5% removal. The performance of modifying agents can be explored as their performance is significantly better than commercial magnetic nanoparticle adsorbents, which can potentially be used in wastewater treatment or recovery of targeted heavy metal ions.

Keywords: Adsorbent; adsorption capacity; microemulsion technique; nanoparticles; oleate-magnetic; silicate-magnetic

ABSTRAK

Penggunaan nanozarah magnetik (MN) untuk pengekstrakan ion logam berat daripada air sisa adalah kaedah yang berpotensi kerana menawarkan kelebihan seperti pemisahan yang mudah, penjanaan semula, kemungkinan pemulihan logam dan pengurangan penjanaan sisa sekunder. Objektif kajian ini adalah untuk menilai keberkesanan dan potensi nanozarah silikat-magnet terubah suai (MNs-SiO) dan nanozarah oleat-magnet (MNs-C-COOH) telah disediakan melalui teknik mikroemulsi W/O keserasian bio. Ciri dan sifat nanozarah besi oksida magnet yang diubah suai telah dikaji oleh mikroskopi elektron pensakanan (SEM), Fourier Transformasi Inframerah (FTIR), X-ray Difraksi (XRD) dan Vibrating-sample magnetometer (VSM). Prestasi penjerap magnet yang diubah suai dinilai untuk penyingkiran ion logam berat terpilih, nikel (Ni^{2+}), mangan (Mn^{2+}) dan plumbum (Pb^{2+}) pada agen pengubah suai dan pH yang berbeza. Didapati bahawa penjerap MNs-SiO adalah bersesuaian terhadap Pb^{2+} (673.4 mg/g) pada pH 3, diikuti oleh Mn^{2+} (544.8 mg/g) dan Ni^{2+} (182.43 mg/g) masing-masing pada pH 7. Penjerap MNs-C-COOH menunjukkan penjerapan Ni^{2+} yang tinggi, iaitu 254 mg/g pada pH 6. Bagi penjerap nanozarah komersial, menunjukkan selektif tinggi terhadap Pb^{2+} , 660.13 mg/g pada pH 6 dan ion-ion lain menunjukkan penyingkiran kurang daripada 5%. Prestasi agen pengubahsuai boleh diterokai kerana prestasinya jauh lebih baik daripada penjerap nanozarah komersial yang berpotensi untuk digunakan sebagai rawatan air sisa atau pemulihan ion logam berat yang disasarkan.

Kata kunci: Kapasiti penjerapan; nanozarah; oleat-magnetik; penjerap; silikat-magnetik; teknik mikroemulsi

INTRODUCTION

Water is an essential element for living things. However, the increased number of contaminants in surface water is due to rapid industrialisation and the massive growth of the human's population (Xu et al. 2012). Industrial activities all over the world are responsible for the presence of various contaminants in water resources (Kalra & Gupta 2019). Heavy metals are one of the main pollutants that cause water contamination (Naseem & Durrani 2021). Advances in wastewater treatment technologies are essential to ensure environmental sustainability. However, eliminating metal ions remains challenging due to their persistence and complexity. Metals such as arsenic can cause skin damage, nerve inflammation, and muscle weakness. Cadmium piles up mainly on the kidney and liver and causes kidney damage and renal failure. Exposure to manganese can cause hallucinations, forgetfulness, and damage to nerves, which can cause the Parkinson's disease (O'Neal & Zheng 2015). Other than that, contact with nickel compounds can harm human health, including contact dermatitis, lung fibrosis, kidney and cardiovascular illness, and respiratory tract cancer. The most common effects of nickel exposure are skin rash and irritation of the nose and sinuses (Burnase, Jaiswal & Barapatre 2022). Several conventional methods and adsorbents exist for the removal of heavy metals. Some disadvantages of its have limited its use in treating effluent. Methods such as membrane separation, electrokinetics, ion exchange, chemical coagulation, electroplating, precipitation, and electroplating are used to remove heavy metals. The disadvantages of these techniques include their high cost, unavailability, generate lots of secondary waste, and poor removal efficiency (Mehdizadeh et al. 2014). De Magalhães et al. stated that one of activated carbon's (AC) weaknesses is it cannot be produced on a large scale as it requires high production costs, as the calcination temperature used can reach 900 °C and above. Other than that, using zeolite as an adsorbent is not ideal due to electrostatic repulsion, anionic species like phosphoric compounds and some heavy metals like chromium and arsenic. Studies showed that adsorption is a highly effective treatment method for wastewater that contains contaminants. Adsorption processes have been used to remove heavy metals in wastewater (Sukmana et al. 2021). Due to its efficiency despite its relatively low cost, the adsorption process has gained widespread attention from it (Rose et al. 2017). However, this non-magnetic adsorbent has disadvantages that cause limitations, such as difficulties in separation from water bodies (Liosis et al. 2021). This study, a newly synthesised material, (MNs-SiO), and (MNs-C-COOH), was introduced to overcome these problems. MNs-SiO and MNs-C-COOH nanoparticles possess an extra feature, which is a magnetism that can tackle the issues with conventional adsorbents as it is easy to separate and regenerate (Hu, Chen & Lo 2005). It also has the potential to recover of valuable metals and helps to reduce the

amount of secondary waste generated. Recent studies have presented iron oxide-based nanoparticles with outstanding properties such as improved adsorption properties, a large surface area and a small particle size (Naseem & Durrani 2021). Iron oxide nanoparticles have a high surface-to-volume ratio, making them an ideal adsorbent with high adsorption capacity and efficiency (Rose et al. 2017). It is also easy to synthesise, coat and modify (Xu et al. 2012). The chemical properties of (MNs-SiO), and (MNs-C-COOH) nanoparticles were characterized in terms of morphology, topography, surface diffractions and functional groups by using Scanning Electron Microscope (SEM), Fourier Transform Infrared (FTIR), X-Ray Diffraction (XRD) and Vibrating-sample magnetometer (VSM) analysis. The focus of this study was to analyse the efficiency of (MNs-SiO), and (MNs-C-COOH) nanoparticles in removing heavy metals by performing the batch tests. Three heavy metals being tested in this study were manganese, nickel, and lead with different contact times as a parameter. The batch test was conducted with a predetermined amount of adsorbent (MNs-SiO) and (MNs-C-COOH) mixed with a heavy metals solution. The concentration was determined by checking the reduction of initial concentration. The data was collected, and the percentage removal and adsorption capacity of heavy metals were calculated.

MATERIALS AND METHODS

MATERIALS

The following chemicals iron chloride tetrahydrate ($\text{FeCl}_2 \cdot 4\text{H}_2\text{O}$), iron chloride hexahydrate ($\text{FeCl}_3 \cdot 6\text{H}_2\text{O}$), manganese chloride (MnCl_2), lead nitrate ($\text{Pb}(\text{NO}_3)_2$), nickel chloride (NiCl_2), and hexane solution were purchased from Merck (Darmstadt, Germany). Aerosol OT-100, ammonium hydroxide (NH_4OH) and 95% ethanol were purchased from Fisher Scientific (New Hampshire, United States). For the commercial magnetic nanoparticles, iron oxide (Fe_3O_4 , <5 nm, >96%) and the modifying agent, oleic acid and silicon oxide, were obtained from Sigma-Aldrich (Missouri, United States). All the chemicals used are analytical grade.

CHARACTERIZATION OF MAGNETIC ADSORBENTS

X-ray Diffraction (XRD) analysis was used to determine the crystallinity of magnetic iron oxide nanoparticles using a Rigaku MiniFlex II Benchtop X-ray Diffraction (XRD). Before running the 'Standard measurement' programme, the samples were attached to the sample holder. To achieve optimum results, the samples must be neatly arranged on the sample holder, and a sample was set between 5° and 80° and operated for 40 min following the procedure. For the Fourier Transform infrared (FTIR) spectroscopy, FTIR-Bruker Invenio-S FTIR Spectrometer was used. The samples were pressed into a pellet using pellet press machine and placed in FTIR spectrometer.

Then, it was exposed to IR beams and recorded in a range of wavelengths (400–4000 cm^{-1}). For the morphology and topography analysis of the modified nanoparticles (MN), the scanning electron microscope (SEM) (JEOL JSM 840) (Peabody, MA, USA) was used. The samples were coated with a thin layer of gold which can prevent charging, lessen heat damage, and enhance the secondary electron signal needed for SEM topographic inspection. The magnetic properties of MN were measured by Vibrating-sample magnetometer (VSM) analysis (Lakeshore, Model: 7404 Series). For the concentration of metal ions, the analysis was performed using Atomic Adsorption Spectroscopy (AAS)(Varian SpectraAA 220FS) at specific wavelengths (Ni^{2+} , 232.0 nm; Mn^{2+} , 279.5 nm; Pb^{2+} , 217.0 nm). The batch experiments were conducted in triplicate.

SYNTHESIS OF MAGNETIC ADSORBENTS

Magnetic iron oxide nanoparticles synthesized by using 0.5 mL of $\text{FeCl}_2 \cdot 6\text{H}_2\text{O}$ and 2.5 mL of $\text{FeCl}_3 \cdot 6\text{H}_2\text{O}$ dissolved in 100 mL distilled water and 2 mL microemulsion template (Hexane, Water and Aerosol OT-100) added. Then, 3.5 mL of ammonium hydroxide (NH_4OH) and 200 mL of distilled water were added. 0.5 mL of the modified agent was added. The mixture was heated for 60 min and then let cool for a while. After cooling, the precipitate was filtered before being washed repeatedly with 95% ethanol and distilled water. The precipitate was dried in an oven at 70 °C for 24 h. Native magnetic iron oxide nanoparticles (MNs-Native) were prepared by the same procedure without a modified agent. The magnetic nanoparticles (MN) were modified with oleic acid (MNs-C-COOH) and silicon oxide (MNs-SiO).

PERFORMANCE EVALUATION OF ADSORBENTS

For the experiment design, to achieve reliability of the results, the manipulative parameters evaluate the modified nanoparticles according to the previous study. Firstly, the performance of native (MNs-native), commercial (MNs-commercial) and modified (MNs-SiO, MNs-C-COOH) nanoparticles as adsorbents were evaluated using different heavy metal ions (Ni^{2+} , Mn^{2+} , Pb^{2+}) by batch adsorption study. About 0.01 g of the adsorbent was added into 250 mL with the concentration of heavy metal ions, 100 mg/mL, in a beaker, separately. The mixtures were mixed and shaken at 150 rpm, and at each time intervals (15, 30, 60, 90, 120, 150, 180, 210, and 240 min), 10 mL of the solution were taken, and the concentration of heavy metal ions was analyzed using AAS. Each analysis was conducted in triplicates and kept in the refrigerator prior to analysis. Then, the effect of different pH (3, 4, 5, 6 and 7) (Allahkarami et al. 2023; Das, Bar & Das 2023; Nassef et al. 2024) during the adsorption process was identified as a chemical parameter which can influence the heavy metal ions adsorption capacity. The procedure was repeated following the previous batch adsorption study, using the

same amount of adsorbent and concentration of heavy metal ions, and running the experiment for 1 h. The final concentration of heavy metal ions was analysed using AAS. The removal efficiency and adsorption capacity can be calculated by the quantity of pollutant adsorbed per unit mass of adsorbent as in Equations (1) and (2), respectively.

$$\%R = \left(\frac{C_0 - C_e}{C_0} \right) \times 100\% \quad (1)$$

where % R is the removal efficiency (%); C_0 is the initial heavy metals ions concentration (mg/mL); and C_e is the equilibrium concentration (mg/mL)

$$q_t = \frac{C_0 - C_e}{m} V \quad (2)$$

where q_t is the amount of heavy metal ions adsorbed per unit mass of adsorbent at time (mg/g); C_0 is the initial heavy metals ions concentration (mg/mL); C_e is the equilibrium concentration (mg/mL); m is the weight of adsorbent (g); and V is the volume of adsorbent (L).

RESULTS AND DISCUSSION

PHYSICOCHEMICAL PROPERTIES OF MAGNETIC ADSORBENTS

The XRD patterns (Figure 1) of unmodified MNs-native and modified MNs-C-COOH nanoparticles were almost identical, confirming the formation of magnetite nanoparticles. The broadening of the peaks in MNs-C-COOH indicates a smaller crystallite size (Chin & Yaacob 2007). The diffraction angle for MNs-C-COOH was at $2\theta = 30.0^\circ$, 36.0° , 57.0° , and 63.0° , which is quite similar to iron oxide (MNs-commercial) lattice, indicating that magnetite nanoparticles were successfully prepared using W/O microemulsion technique (Abdelbasir et al. 2021). Figure 2 shows representative SEM images of magnetite nanoparticles of native MNs (a), functionalized MNs-C-COOH (b), and MNs-SiO (c). The SEM image of the native 2(a), shows a rough and irregular surface morphology. The particles also exhibit agglomeration, which is likely due to strong magnetic interactions between the individual particles (Bandar, Anbia & Salehi 2021). In Figure 2(b), the MNs-C-COOH show a more uniform and less agglomerated appearance compared to the native MNs. The functionalization with carboxyl groups seems to weaken the magnetic interactions, leading to a better dispersion of the particles. The presence of the carboxyl group coating probably contributes to a smoother and more consistent surface structure, which increases the stability of the particles and the adsorption potential for certain metal ions. Oleic acid is often used as a capping agent to create a protective monolayer that is tightly bound to the surface of the nanoparticles, resulting in a uniform monodisperse

surface (Mengesha, Hoerres & Mahajan 2022). Surface features indicate the surface area volume, which is related to the potential active site for metal ion attachment. Rough surfaces indicate the presence of cracks, which reflect a large surface area compared to smooth surfaces (Germanos et al. 2020). This property also contributes to the performance of the adsorption capacity for the desired metal ions (Ibrahim et al. 2024).

The possible chemical bonds in (MNs-SiO) and (MNs-C-COOH) iron oxide was investigated by examining the FTIR characteristics peaks $4000 - 400 \text{ cm}^{-1}$ to match the corresponding chemical bonds. Figure 3 shows the FTIR spectra of native magnetic iron oxide nanoparticles (a), magnetic iron oxide nanoparticles modified with oleic acid (b) and magnetic iron oxide modified with silicon oxide (c). The peaks at 2922.03 and 2857.91 cm^{-1} in MNs-native and 2917.86 cm^{-1} and 2849.17 cm^{-1} in MNs-C-COOH correspond to asymmetric and symmetric CH_2 stretching, respectively, with a slight shift due to the addition of oleic acid (Mahdavi et al. 2013). The band at 1524.13 cm^{-1} ($\nu_{\text{as}} : \text{COO}$) (curve (b)) in MNs-C-COOH indicates the presence of oleate ion immobilized on the magnetite surface. Mahdavi et al. (2013) classify the interactions between the carboxylate head and the metal atom into three types based on their research and other studies on carboxylates; Structure I: unidentate complex where one metal ion is binding with one carboxylic oxygen atom, Structure II: bidentate complex (chelating) where one metal ion is binding with two carboxylate oxygens, and Structure III: bridging complex where two metal ions are binding with two carboxylate oxygens.

The peaks at 890.30 , 1037.36 , and 1205.51 cm^{-1} were attributed to deformations of the Fe-OH group, while the band at 690.18 cm^{-1} and 1080.45 cm^{-1} attributed to the Fe-O-Si stretching vibration and confirmed the adsorption of the silane polymer (Si-O-Si) on the magnetite surface (Storozhuk & Iukhymenko 2019). The magnetic adsorbents, iron oxide-based materials, tend to damage under acidic conditions. Adding a template such as a silicate coating can seal the outer shell and protect the inner magnetite core from remaining stable in acidic conditions. Silica coating will enhance the stability of magnetite. The hydroxyl groups on the surface of the SiO_2 coating shell offer numerous reaction sites for the covalent attachment to the magnetic composites. These strong metal-chelating properties produce functionalized magnetite nanoparticles that are reliable in removing various heavy metal ions, such as Cu^{2+} , Co^{2+} , Pb^{2+} , Cr^{6+} , and Fe^{3+} , from the aqueous solutions (Meng et al. 2018).

VSM analysis (Figure 4, Table 1) discovered high magnetization (Ms) values for MNs-Commercial (55.5437 emu/g), MNs-Native (53.4281 emu/g) and MNs-C-COOH (54.274 emu/g), indicating their strong magnetic properties. In particular, MNs-C-COOH exhibited a higher Ms value than MNs-native, indicating the robust magnetic properties of the iron oxide nanoparticles after carboxyl functionalization. In contrast, MNs-SiO

showed a relatively low Ms value of 27.297 emu/g . The retentivity magnetization (Mr) values followed a similar trend, with MNs-commercial (4.2175 emu/g), MNs-Native (3.2175 emu/g), MNs-C-COOH (3.3507 emu/g) and MNs-SiO (1.9651 emu/g), respectively. These results show that the magnetization (Ms) is directly proportional to the retentivity magnetization (Mr), highlighting the magnetic behaviour of the nanoparticles. However, the coercivity values exhibited an inverse relationship with the magnetization values, suggesting that higher magnetization leads to lower coercivity. This finding is consistent with the expected behaviour of magnetic nanoparticles, where increasing particle size generally leads to increased magnetization and lower coercivity. The magnetization results indicate MNs-C-COOH has a high-value proposition to MNs-native, suggesting iron oxide's inherent strong magnetic characteristics. While MNs-SiO exhibits a lower value of 27.297 emu/g . The retentivity (Mr) of magnetization was recorded values for MNs-commercial, 4.2175 emu/g , MNs-native, 3.2175 emu/g , MNs-C-COOH, 3.3507 emu/g , and MNs-SiO, 1.9651 emu/g , respectively. It can be concluded that the magnetization (Ms) is directly proportional to the retentivity (Mr) of magnetization, which highlights the magnetism of MNs. The coercivity values show each type of MN's inversely proportional magnetization value. The trend indicates that as the magnetization values of MNs increase, the coercivity values tend to decrease.

PERFORMANCE OF (MNS-SIO) AND (MNS-C-COOH) NANOPARTICLES AS HEAVY METALS IONS ADSORBENT

The adsorption of Mn^{2+} , Ni^{2+} and Pb^{2+} by the different MNs was investigated over time (Figure 5). MNs-natives showed rapid adsorption of all heavy metal ions within the first 15 min, followed by a gradual increase until maximum capacity was reached after 60 min (Mn^{2+}) and 120 min (Pb^{2+}). The order of preference was $\text{Mn}^{2+} > \text{Pb}^{2+} > \text{Ni}^{2+}$. For MNs-C-COOH, Ni^{2+} adsorption gradually increased between 15 and 60 min and then decreased due to saturation (Geroeeyan, Niazi & Konož 2021). Mn^{2+} remained constant after 15 min, with the preferred order being $\text{Ni}^{2+} > \text{Mn}^{2+} > \text{Pb}^{2+}$. MNs-SiO showed a high uptake of Mn^{2+} and Ni^{2+} compared to Pb^{2+} in the first 60 min, followed by a decrease after 90 min due to limited adsorption sites. The decreasing tendencies of the heavy metals towards the adsorbent were: MNs-native; ($\text{Mn}^{2+} > \text{Pb}^{2+} > \text{Ni}^{2+}$), MNs-C-COOH, ($\text{Ni}^{2+} > \text{Mn}^{2+} > \text{Pb}^{2+}$), MNs-SiO, ($\text{Mn}^{2+} > \text{Ni}^{2+} > \text{Pb}^{2+}$), and MNs-commercial, ($\text{Mn}^{2+} > \text{Pb}^{2+} > \text{Ni}^{2+}$). Due to the similar chemical structure of native MNs (MNs-native) and commercial (MNs-commercial), the trends in heavy metal adsorption were quite similar (Figure 6(a) and 6(b)). However, the differences in heavy metal adsorption on modified MNs were observed due to the functionalization of the adsorbents. Metal ion Pb^{2+} is the most preferable metal ions to be absorb compared to other metals due to its

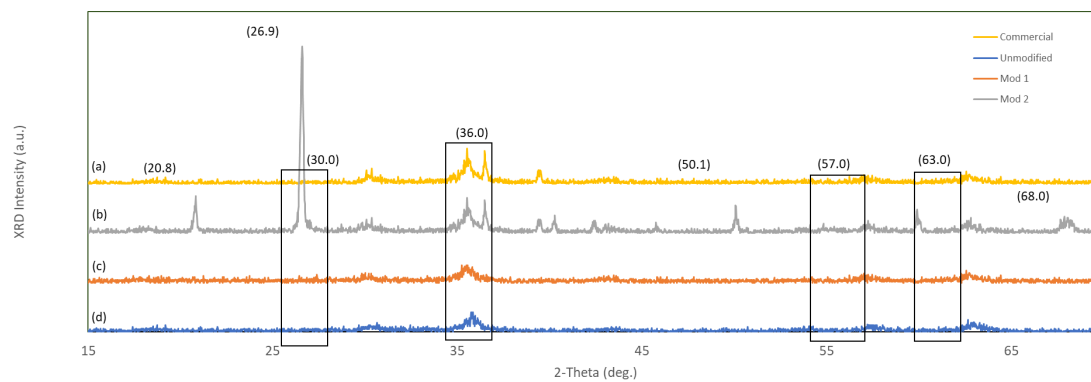


FIGURE 1. XRD patterns of magneticnanoparticles (MNs) (a)MNs-commercial, (b) MNs-SiO, (c) MNs-C-COOH and (d) MNs-native

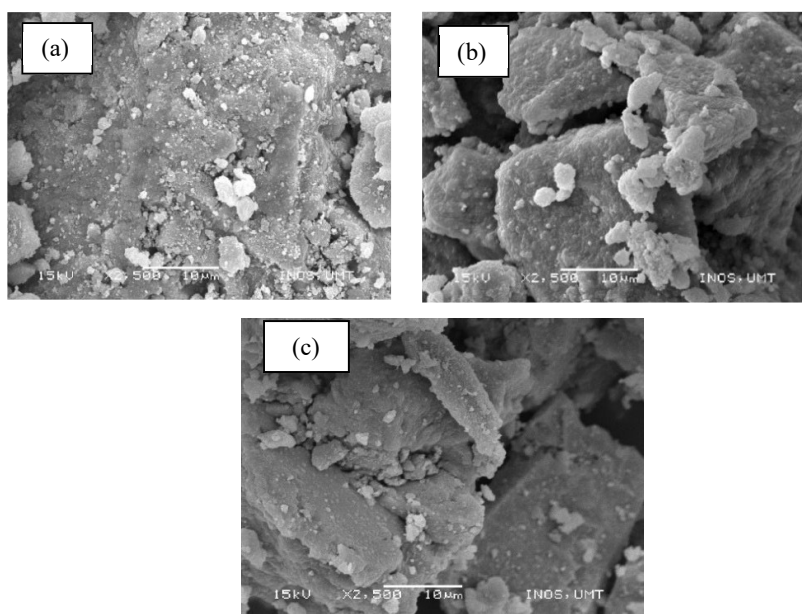


FIGURE 2. SEM micrograph at x 2,500 magnifications of magnetic nanoparticles (MNs) (a) MNs-native, (b) MNs-C-COOH, and (c) MNs-SiO

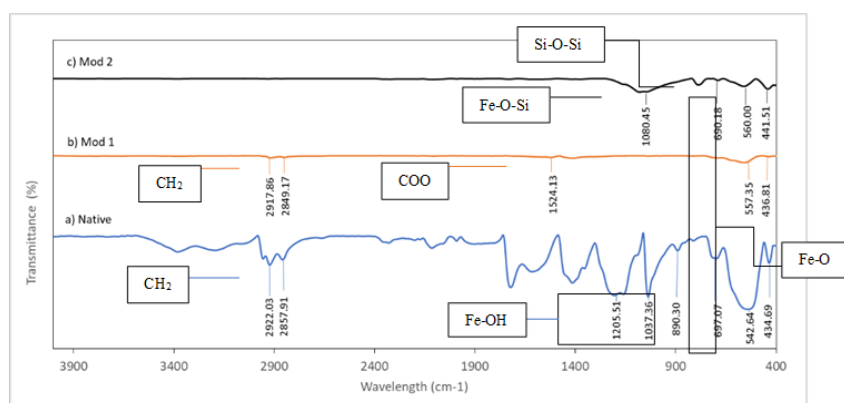


FIGURE 3. FTIR spectra of magnetic nanoparticles (a) MNs-SiO, (b) MNs-C-COOH, and (c) MNs-native

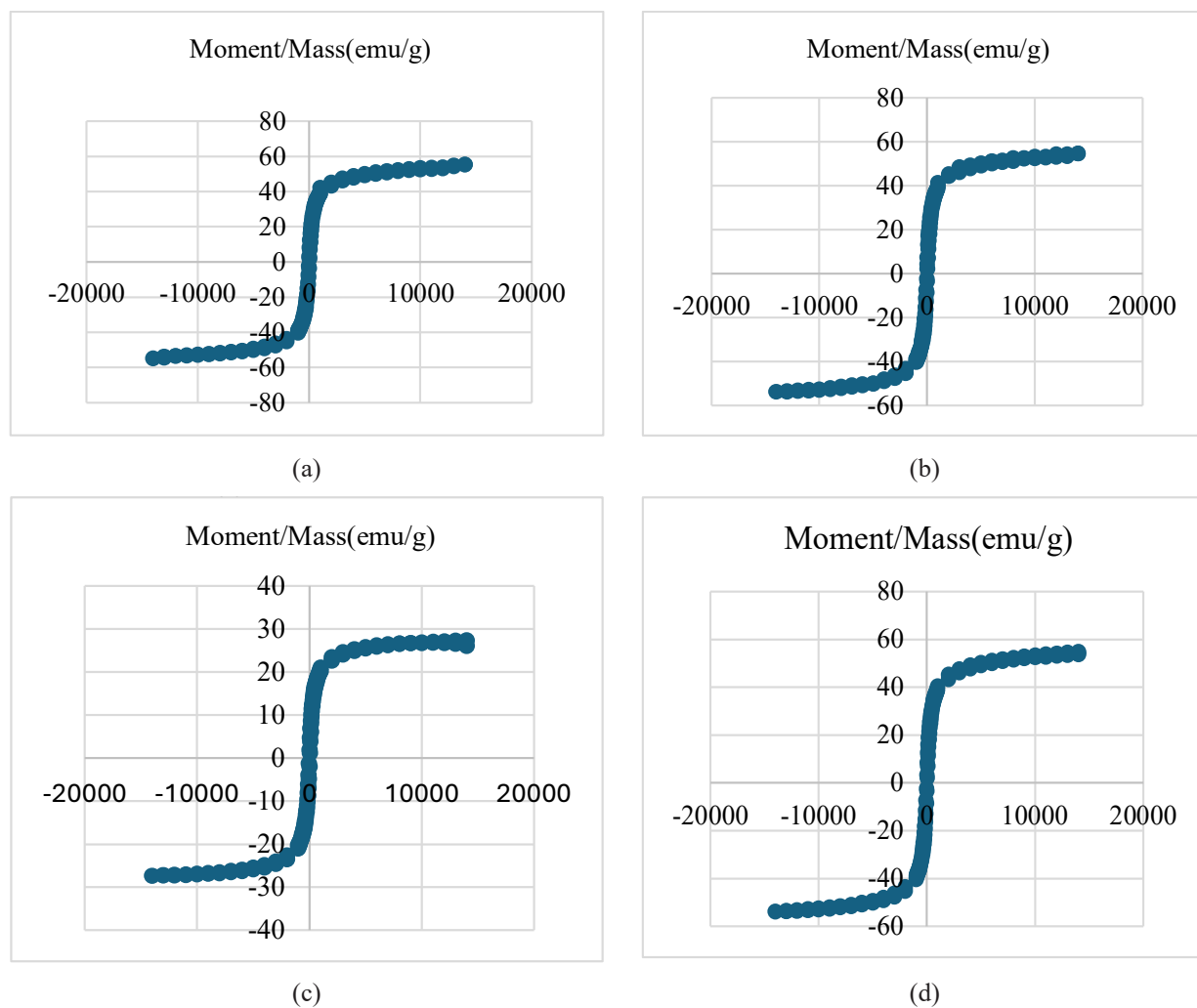
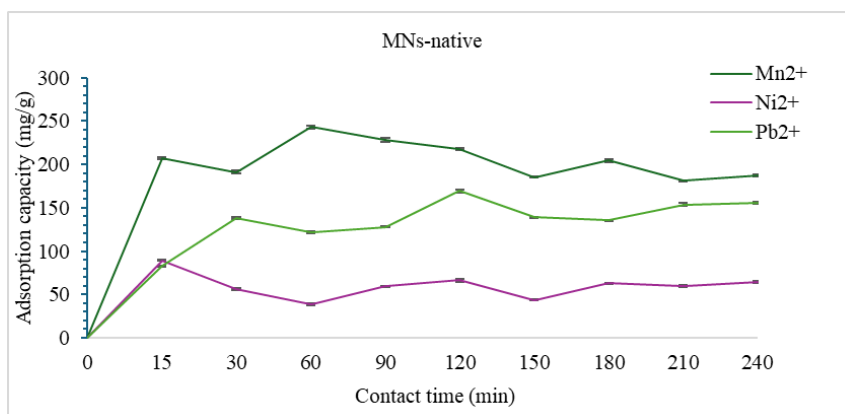


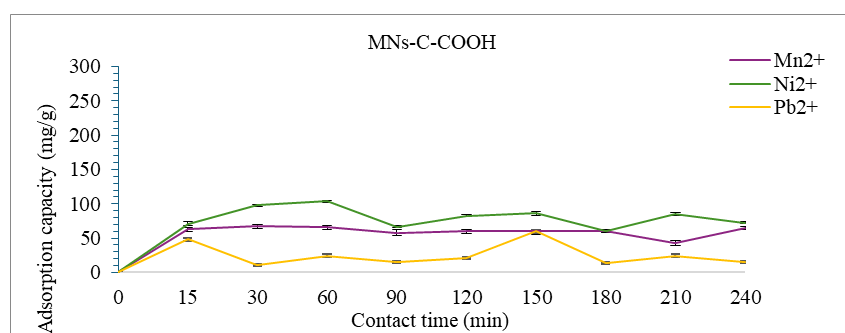
FIGURE 4. The plot of VSM analysis of magnetic nanoparticles (MNs)
 (a) MNs-commercial, (b) MNs-native, (c) MNs-C-COOH, and
 (d) MNs-SiO

TABLE 1. The analytical data of VSM analysis for magnetic nanoparticles (MNs)

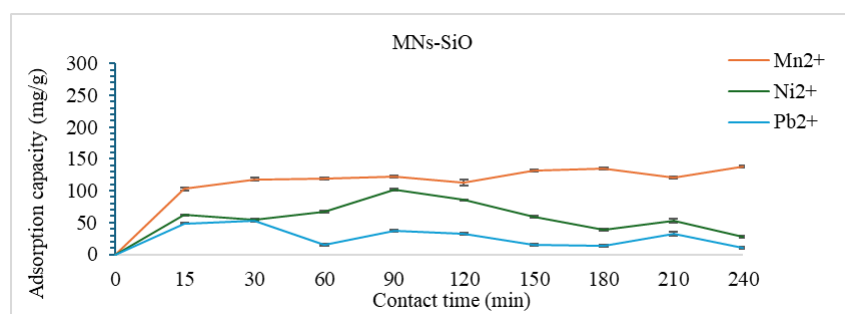
Samples	Magnetization, M_s (emu/g)	Coercivity, H_{ci} (G)	Retentivity, M_r (emu/g)
MNs-commercial	55.5437	21.751	4.2175
MNs-native	53.4281	24.352	3.2175
MNs-C-COOH	54.274	24.113	3.3507
MNs-SiO	27.297	25.237	1.9651



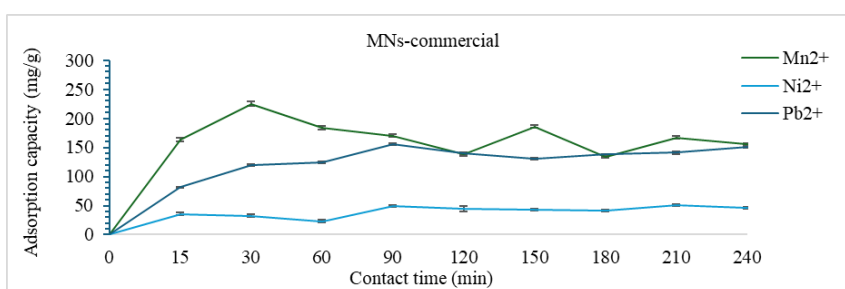
(a)



(b)



(c)



(d)

FIGURE 5. The adsorption capacity of magnetic nanoparticles (MNs) effect of contact time (a) native MNs, (b) modified MNs with oleic acid (MNs-C-COOH), (c) modified MNs with silicon oxide (MNs-SiO), and (d) commercial MNs (MNs-commercial)

larger ionic radius and high affinity towards the functional groups, particularly carboxyl and hydroxyl of active site on magnetite adsorbent surfaces (Zhou et al. 2024). At different pH values of the solution, high adsorption capacity of metal ions was obtained by modified MNs with oleic acid (MNs-C-COOH), compared to the modified MNs with silicon oxide (MNs-SiO). Figure 6(c) shows that the adsorbent of MNs-C-COOH tends to adsorb Pb^{2+} at pH 4 and Ni^{2+} and Mn^{2+} at pH, while the adsorbents (MNs-SiO) exhibit lower adsorption towards selected metal ions and has only a higher value at pH 6, which is a slightly acidic environment. The influence of pH on the adsorption capacity of heavy metals by functionalized iron oxides is significant (Garg et al. 2023; Lei et al. 2023). The pH controls the surface charge of the adsorbent material and the speciation of heavy metal ions in the solution (Yang et al. 2022). It also influences the complexation behaviour of the functional groups on the adsorbent surface (Figure 6), with soft Lewis's base groups favouring

dipole-dipole interactions and hard Lewis base groups favoring cation exchange (Rafiq, Wongrod & Vinitnantharat 2023). As shown in the Figure 7, the MNs-native and MNs-commercial tend to adsorb Pb to a high extent, and adsorption increases when the pH rises to a neutral value, as it is similar to functionalized surface of the adsorbent ($FeCl_3$). In a previous study, the slight changes in pH affect heavy metal removal efficiency. At low pH values, between 2 and 3, the removal rate slowed compared to when the values increased. Thus, the removal percentage rapidly increased from 17 to 92% as the pH values risen from 3 to 6 (Khan et al. 2021). A similar response on pH values in research using $Fe_2O_3-Al_2O_3$ nanocomposite fibre, due to competition between H^+ ions and metal ions for the available adsorption sites. As a result, the removal effectiveness is poor at low pH (Mahapatra, Mishra & Hota 2013). Between pH 4 and 8, arsenic removal reached 100% of adsorption and decreased later to 91.12% at pH 10 and 77.25% at pH 12 (Mostafa et al. 2011).

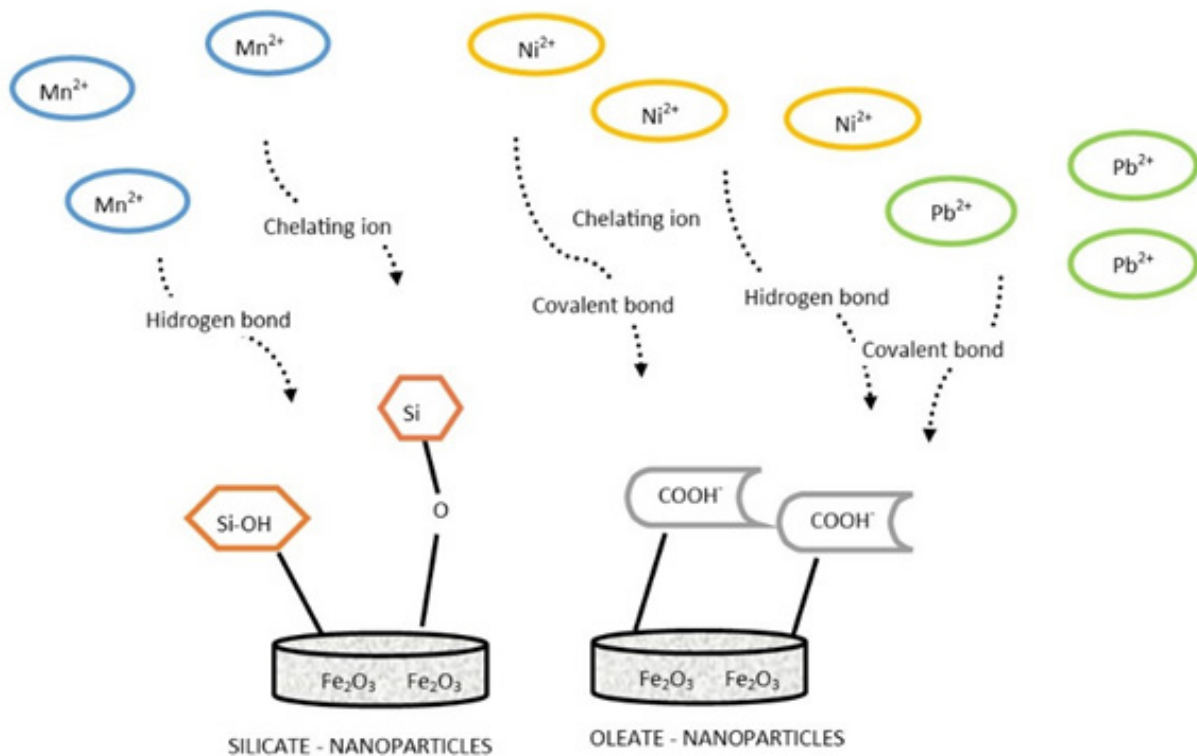
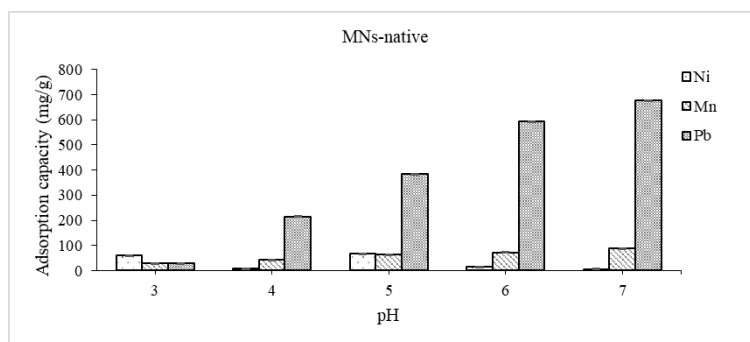
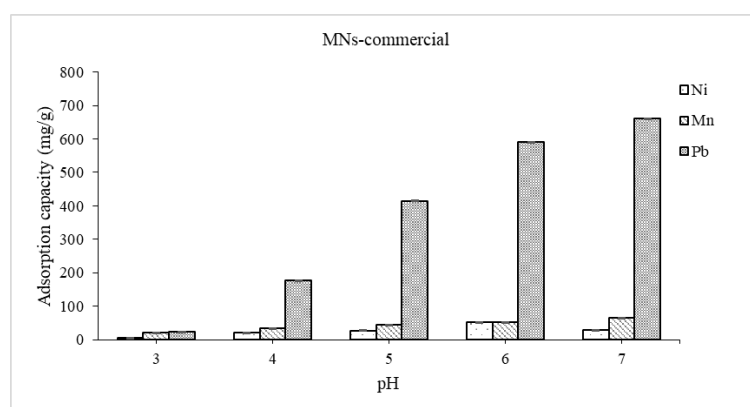


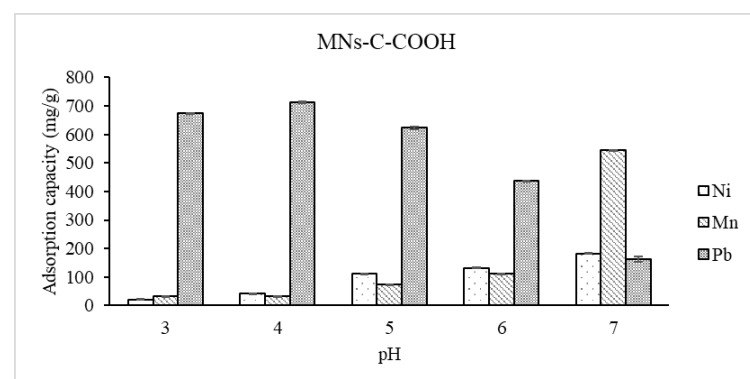
FIGURE 6. Potential active sites on silicate and oleate nanoparticles, and their possible chemical interactions with metal ions



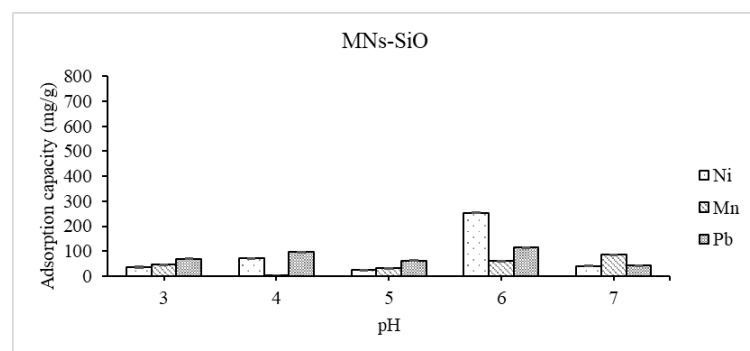
(a)



(b)



(c)



(d)

FIGURE 7. The adsorption capacity of magnetic nanoparticles (MNs) effect of pH (a) native MNs, (b) commercial MNs (MNs-commercial), (c) modified MNs with oleic acid (MNs-C-COOH), and (d) modified MNs with silicon oxide (MNs-SiO)

CONCLUSION

The silicate- and oleate-(MNs-SiO) and (MNs-C-COOH) nanoparticles successfully adsorbed and removed specific metal ions from solutions, demonstrating that surface modification has been achieved. The findings of this study highlight the significance of selecting the appropriate modifying agent, as it controls the formation of active sites on the adsorbent's surfaces with desired metal ions. The pH of the metal ion solution must also be considered, as it influences the ionization and chemical interaction between the adsorbent and the metal ions. It suggests that surface modification of magnetic nanoparticles offers a viable approach to address water pollution caused by various contaminants. The effectiveness of the treatment can be achieved by considering the appropriate modifying agents and understanding the possibility of key chemical interactions. Additionally, the adsorbent regeneration assessment should be regarded to determine the reusability and magnetic properties of these nanoparticles that appeal to industry applications. The surface modification of magnetic nanoparticles improves their efficiency, selectivity and stability. In addition, magnetic properties are known as ease of use and can be reused, making this future adsorbent fulfil industrial demand as its practicality and cost savings.

ACKNOWLEDGMENTS

The authors would like to thank Universiti Malaysia Terengganu for the financial support under Talent and Publications Enhancement Research Grant (TAPE-RG), grant number TAPERG/2021/UMT/528.

REFERENCES

- De Magalhães et al.
- Abdelbasir, S.M., Elseman, A.M., Harraz, F.A., Ahmed, Y.M.Z., El-Sheikh, S.M. & Rashad, M.M. 2021. Superior UV-light photocatalysts of nano-crystalline (Ni or Co) FeWO_4 : structure, optical characterization and synthesis by a microemulsion method. *New Journal of Chemistry* 45(6): 3150-3159.
- Allahkarami, E., Soleimanpour Moghadam, N., Jamrotbe, B. & Azadmehr, A. 2023. Competitive adsorption of Ni(II) and Cu(II) ions from aqueous solution by vermiculite-alginate composite: Batch and fixed-bed column studies. *Journal of Dispersion Science and Technology* 44(8): 1402-1412.
- Bandar, S., Anbia, M. & Salehi, S. 2021. Comparison of MnO_2 modified and unmodified magnetic Fe_3O_4 nanoparticle adsorbents and their potential to remove iron and manganese from aqueous media. *Journal of Alloys and Compounds* 851: 156822.
- Burnase, N., Jaiswal, S. & Barapatre, A. 2022. Metal toxicity in humans associated with their occupational exposures due to mining. In *Medical Geology in Mining*, edited by Randive, K., Pingle, S., Agnihotri, A. Springer Geology. pp. 127-186.
- Chin, A.B. & Yaacob, I.I. 2007. Synthesis and characterization of magnetic iron oxide nanoparticles via w/o microemulsion and Massart's procedure. *Journal of Materials Processing Technology* 191(1): 235-237.
- Das, A., Bar, N. & Das, S.K. 2023. Adsorptive removal of Pb(II) ion on Arachis hypogaea's shell: Batch experiments, statistical, and GA modeling. *International Journal of Environmental Science and Technology* 20(1): 537-550.
- Garg, R., Garg, R., Khan, M.A., Bansal, M. & Garg, V.K. 2023. Utilization of biosynthesized silica-supported iron oxide nanocomposites for the adsorptive removal of heavy metal ions from aqueous solutions. *Environmental Science and Pollution Research* 30: 81319-81332.
- Germanos, G., Youssef, S., Farah, W., Lescop, B., Rioual, S. & Abboud, M. 2020. The impact of magnetite nanoparticles on the physicochemical and adsorption properties of magnetic alginate beads. *Journal of Environmental Chemical Engineering* 8(5): 104223.
- Geroeeyan, A., Niazi, A. & Konozi, E. 2021. Removal of basic orange 2 dye and Ni^{2+} from aqueous solutions using alkaline-modified nanoclay. *Water Science and Technology* 83(9): 2271-2286.
- Hu, J., Chen, G. & Lo, I.M.C. 2005. Removal and recovery of Cr(VI) from wastewater by maghemite nanoparticles. *Water Research* 39(18): 4528-4536.
- Ibrahim, G.M., Alshahrani, S.M., Alosaimi, E.H., Alshahrani, W.A., El-Gammal, B., Fawzy, A., Alqarni, N., Elhouichet, H. & Safaa, H.M. 2024. Adsorption mechanism elucidation of anionic congo red onto modified magnetic nanoparticle structures by quantum chemical and molecular dynamics. *Journal of Molecular Structure* 1298(Part 1): 13992.
- Kalra, A. & Gupta, A. 2019. Recent advances in decolourization of dyes using iron nanoparticles: A mini review. *Materials Today: Proceedings* 36: 689-696.
- Khan, J., Lin, S., Nizeyimana, J.C., Wu, Y., Wang, Q. & Liu, X. 2021. Removal of copper ions from wastewater via adsorption on modified hematite ($\alpha\text{-Fe}_2\text{O}_3$) iron oxide coated sand. *Journal of Cleaner Production* 319: 128687.
- Lei, T., Jiang, X., Zhou, Y., Chen, H., Bai, H., Wang, S. & Yang, X. 2023. A multifunctional adsorbent based on 2,3-dimercaptosuccinic acid/dopamine-modified magnetic iron oxide nanoparticles for the removal of heavy-metal ions. *Journal of Colloid and Interface Science* 636: 153-166.
- Liosis, C., Papadopoulou, A., Karvelas, E., Karakasidis, T.E. & Sarris, I.E. 2021. Heavy metal adsorption using magnetic nanoparticles for water purification: A critical review. *Materials* 14(24): 7500.
- Mahapatra, A., Mishra, B.G. & Hota, G. 2013. Electrospun $\text{Fe}_2\text{O}_3\text{-Al}_2\text{O}_3$ nanocomposite fibers as efficient adsorbent for removal of heavy metal ions from aqueous solution. *Journal of Hazardous Materials* 258-259: 116-123.

- Mahdavi, M., Ahmad, M. Bin, Haron, M.J., Namvar, F., Nadi, B., Ab Rahman, M.Z. & Amin, J. 2013. Synthesis, surface modification and characterisation of biocompatible magnetic iron oxide nanoparticles for biomedical applications. *Molecules* 18(7): 7533-7548.
- Mehdizadeh, S., Sadjadi, S., Ahmadi, S.J. & Outokesh, M. 2014. Removal of heavy metals from aqueous solution using platinum nanoparticles/Zeolite-4A. *Journal of Environmental Health Science and Engineering* 12: 7.
- Meng, C., Zhikun, W., Qiang, L., Chunling, L., Shuangqing, S. & Songqing, H. 2018. Preparation of amino-functionalized $\text{Fe}_3\text{O}_4@\text{mSiO}_2$ core-shell magnetic nanoparticles and their application for aqueous Fe^{3+} removal. *Journal of Hazardous Materials* 341: 198-206.
- Mengesha, A., Hoerres, A. & Mahajan, P. 2022. Cytocompatibility of oleic acid modified iron oxide nanoparticles. *Materials Letters* 323: 132528.
- Mostafa, M.G., Chen, Y.H., Jean, J.S., Liu, C.C. & Lee, Y.C. 2011. Kinetics and mechanism of arsenate removal by nanosized iron oxide-coated perlite. *Journal of Hazardous Materials* 187(1-3): 89-95.
- Naseem, T. & Durrani, T. 2021. The role of some important metal oxide nanoparticles for wastewater and antibacterial applications: A review. *Environmental Chemistry and Ecotoxicology* 3: 59-75.
- Nassef, H.M., Al-Hazmi, G.A.A.M., Alayyafi, A.A.A., El-Desouky, M.G. & El-Bindary, A.A. 2024. Synthesis and characterization of new composite sponge combining of metal-organic framework and chitosan for the elimination of Pb(II), Cu(II) and Cd(II) ions from aqueous solutions: Batch adsorption and optimization using Box-Behnken design. *Journal of Molecular Liquids* 394: 123741.
- O'Neal, S.L. & Zheng, W. 2015. Manganese toxicity upon overexposure: A decade in review. *Current Environmental Health Reports* 2(3): 315-328.
- Rafiq, S., Wongrod, S. & Vinitnantharat, S. 2023. Adsorption kinetics of cadmium and lead by biochars in single- and bisolute brackish water systems. *ACS Omega* 8(48): 45262-45276.
- Rose, L.C., Suhaimi, H., Mamat, M. & Lik, T.Z. 2017. Synthesis and characterization of oleic acid surface modified magnetic iron oxide nanoparticles by using biocompatible w/o microemulsion for heavy metal removal. *AIP Conference Proceedings* 1885: 020113.
- Storozhuk, L. & Iukhymenko, N. 2019. Iron oxide nanoparticles modified with silanes for hyperthermia applications. *Applied Nanoscience (Switzerland)* 9(5): 889-898.
- Sukmana, H., Bellahsen, N., Pantoja, F. & Hodur, C. 2021. Adsorption and coagulation in wastewater treatment – Review. *Progress in Agricultural Engineering Sciences* 17(1): 49-68.
- Xu, P., Zeng, G.M., Huang, D.L., Feng, C.L., Hu, S., Zhao, M.H., Lai, C., Wei, Z., Huang, C., Xie, G.X. & Liu, Z.F. 2012. Use of iron oxide nanomaterials in wastewater treatment: A review. *Science of the Total Environment* 424: 1-10.
- Yang, Z., Ma, J., Liu, F., Zhang, H., Ma, X. & He, D. 2022. Mechanistic insight into pH-dependent adsorption and coprecipitation of chelated heavy metals by *in-situ* formed iron (oxy)hydroxides. *Journal of Colloid and Interface Science* 608(Part 1): 864-872.
- Zhou, C., Li, B., Li, Y., Zhao, J., Mei, Q., Wu, Y., Chen, Y., Li, M. & Fan, Y. 2024. A review of graphene oxide-based adsorbents for removing lead ions in water. *Journal of Environmental Chemical Engineering* 12(1): 111839.

*Corresponding author; email: hafiza.ilyana@umt.edu.my